

Significance of Ratcheting in Seismic Analyses

Dan Eggers¹ and Mirza M. Irfan Baig²

¹ Associate Principal, Simpson Gumpertz & Heger Inc., USA

² Senior Staff II, Simpson Gumpertz & Heger Inc., USA

ABSTRACT

Simplified seismic analyses consider inelastic dynamic behavior based on scaling of elastic dynamic analyses. The simplified analyses are typically based on an assumption of relatively symmetrical hysteresis behavior. For systems with a constant load from soil pressure or subjected to gravity load in addition to the seismic load, inelastic behavior can occur in one direction without a corresponding effect in the other. This ratcheting effect can increase the total displacement and result in unacceptable performance earlier than may be predicted by analyses that do not account for the effect.

Non-linear time history response analyses were performed for a suite of time histories, systems with a large range of system fundamental frequencies, a full elasto-plastic hysteresis loop and pinched concrete hysteresis model, and various levels of seismic and non-seismic demand. The analyses show that ratcheting behavior is affected by each of the factors examined. For the cases studied, the ratcheting effect resulted in deformations more than twice that predicted by the analysis of a comparable seismic-only non-ratcheting analysis.

This study identifies the importance of considering ratching effects when predicting unacceptable performance of a system based on allowable ductility. The authors propose a modification to inelastic energy absorption factors to account for the effect of ratcheting. Time history response analyses can also be used to calculate a more precise estimation of total deformation or other complex response parameters.

INTRODUCTION

Analysis and design of structures commonly addresses the lateral seismic response of structures and accounts for nonlinear effects through a variety of means. Nonlinear response can be modelled directly using nonlinear finite element analysis software and careful modelling of material and system response including hysteresis behavior. Nonlinear response can also be addressed in design through the use of linear elastic analyses combined with inelastic energy absorption factors, F_{μ} , used in ASCE/SEI 43-05 or through response modification coefficients, R , used in ASCE 7. The factors provided in these standards to address nonlinear response are based on analyses for lateral loads in a generally symmetric loading condition. Presence of non-seismic load acting in the same direction as the seismic load alters the seismic response. This non-seismic load can occur through a lateral load such as unbalanced soil or hydrostatic fluid loads or vertically due to gravity where seismic and gravity load can add to the dynamic loading. If the system response is forced into a nonlinear range, the combination of seismic and non-seismic demands can result in nonlinear response in one direction without a corresponding unloading in the other direction. The resulting nonlinearities are then biased in one direction creating a ratcheting effect. The ratcheting response increases the system ductility or displacement demand beyond that expected when neglecting ratcheting effects. However, a system designed to resist significant non-seismic demand in addition to seismic demand will have greater overall capacity to resist seismic induced nonlinearity than a corresponding system designed for seismic demands only. Therefore, the combined effect of non-seismic demand and ratcheting on the system ductility demand is not inherently known.

This paper examines the effect of ratcheting on the ductility demands for systems for varying levels of non seismic demand. The analyses are based on the ASCE/SEI 43-05 design approach. In this paper, the authors first identify the potential significance of ratcheting and subsequently examine a suite of analyses performed to identify a modification factor for the ASCE/SEI 43-05 inelastic energy absorption factors. These factors are intended to allow designers to consider ratcheting to achieve an 84th percentile non-exceedance of the ductility demand of systems designed without ratcheting.

ANALYSIS APPROACH

In order to examine the effect of ratcheting on non-linear ductility demand, a series of nonlinear single degree of freedom (SDOF) analyses were performed. The analyses considered time history acceleration input motions, a selected nonlinear system behavior (hysteresis model), and response calculation considering design for seismic-only demands and seismic demands plus non-seismic demand. In all cases analyzed, the seismic demand (D_S), non-seismic demand (D_{NS}), inelastic energy absorption factor (F_μ), and design capacity (C) are balanced in accordance with ASCE/SEI 43-05 Eq. 5-1a:

$$C = D_{NS} + D_S/F_\mu \quad \text{Eq. 1.}$$

The analyses for comparison of response due to seismic-only demand to the response due to seismic plus non-seismic demand considered identical system properties. Therefore, the seismic plus non-seismic demand cases considered lower seismic demand than the corresponding seismic-only cases to compensate for the need to also resist non-seismic demand.

Two system hysteresis models were considered in the analyses. The first was a full hysteresis model using bi-linear elasto-plastic behavior. Unloading and reloading followed the same slope as the initial loading and the Baughinger effect was included through full kinematic hardening. The second hysteresis model was intended to represent a generic pinched concrete hysteresis based on the Ibarra-Medina-Krawinler (IMK) pinching model (Ibarra et. al. 2005). The IMK model allows for pinched hysteresis, strength reduction, strength degradation due to repeated cycles, and unloading stiffness degradation. However, strength reduction, strength degradation, and unloading stiffness degradation were not considered for this study and parameters κ_f and κ_d (coefficients for locating the pinch point (Ibarra et. al. 2005)) were set at 0.3 and 0.4 respectively. All the analyses for this study used a backbone curve with capacity (C) at 0.9 nominal yield (F_y), mean yield (Q_y) at 1.25 C , and a post yield stiffness equal to 1% of initial stiffness (k) (Figure 1). These parameters are consistent with those described in Mertz, G.E., and Houston, T. (2001), "Force reduction factors for the structural design and evaluation of facilities containing nuclear and hazardous materials" (Mertz and Houston 2001).

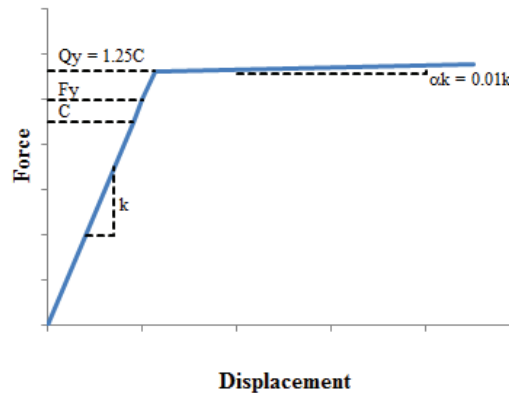


Figure 1: Nonlinear Backbone Curve

Figures 2 through 5 show example hysteresis responses for both full and pinched hysteresis cases for seismic-only and corresponding seismic plus non-seismic demands.

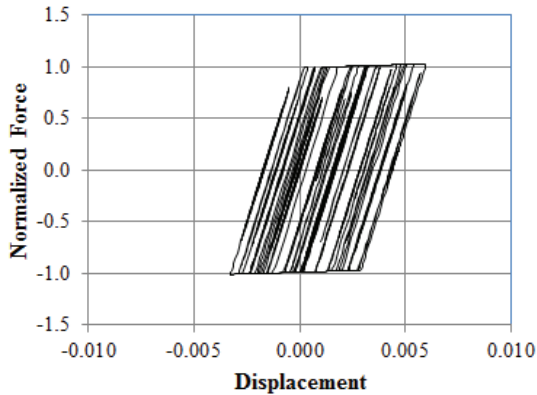


Figure 2: Hysteresis for Full Hysteresis Model, Seismic-Only Loading

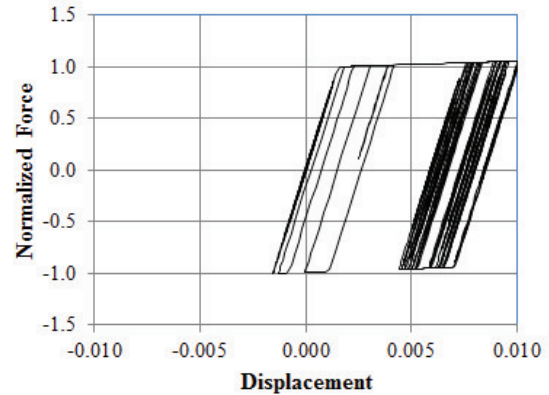


Figure 3: Hysteresis for Full Hysteresis Model, $D_{NS} = 0.1C$

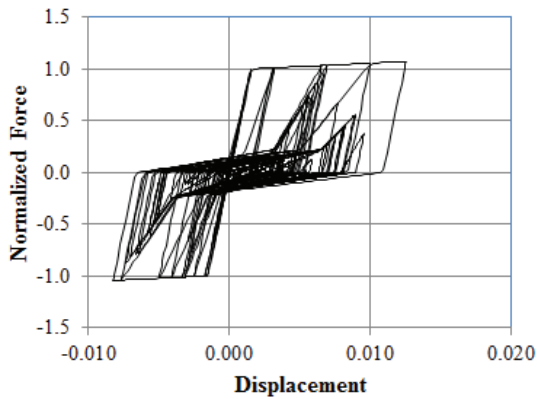


Figure 4: Hysteresis for Pinched Hysteresis Model, Seismic-Only Loading

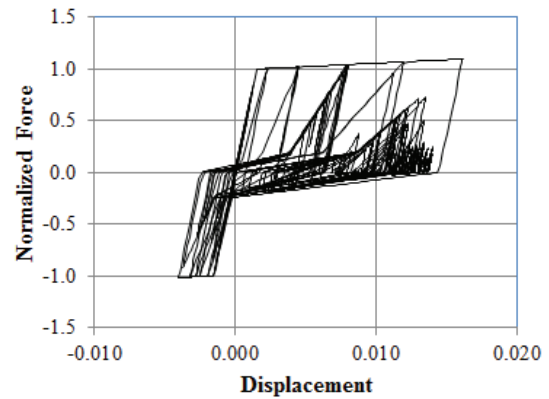


Figure 5: Hysteresis for Pinched Hysteresis Model, $D_{NS} = 0.1C$

EXAMINATION OF EFFECT OF RATCHETING ON DISPLACEMENTS

To calculate the effect of ratcheting on displacement, the system was first designed for seismic-only demand in accordance with Equation 1 for zero non-seismic demand, the selected F_{μ} , and the input time history spectral acceleration at the system elastic frequency. Without changing the system characteristics (yield point or elastic frequency), a non-seismic (static) demand was added and the seismic demand was scaled down to achieve the same total demand per Equation 1, accounting for the selected F_{μ} . Non-seismic demand ratio (γ_{ns}) is defined as the non-seismic demand (D_{NS}) divided by the capacity (C):

$$\gamma_{ns} = D_{NS} / C \quad \text{Eq. 2.}$$

Therefore, for a given non-seismic demand ratio, the remaining capacity is $C \times (1 - \gamma_{ns})$ and the seismic demand, $D_S = C \times (1 - \gamma_{ns}) \times F_{\mu}$.

SDOF nonlinear response history analyses were performed for each loading condition and the resulting peak deflection from the seismic-only case (δ_0) was compared to the peak deflection from the seismic plus non-seismic case (δ) to observe the effect on total system ductility demand. This approach is based on the assumption that the seismic-only analysis produces the desired deflection for the selected value of F_μ . If the system ductility demands are increased by the addition of non-seismic demand, the ratio δ/δ_0 is greater than 1.0, indicating that ratcheting produces an undesirable result. The analyses were performed for over 1500 cases considering:

- Six different earthquake records (4 recorded, 2 artificial)
- Ten levels of non-seismic demand as a percentage of the total demand
- Three values of F_μ : 1, 3, and 5
- Nine different frequencies of the elastic system
- One damping level: 4%
- The backbone curve identified in Figure 1.

Note that ASCE/SEI 43-05 provides adjustment for F_μ to account for systems that have a predominant structural response at a frequency above the peak spectral frequency (see ASCE 43-05 Eq. 5-3). However, in this calculation it was assumed that the values for F_μ have already been adjusted for this effect in all cases. Therefore, the direct comparison of the resulting deflections can be used.

Four non-scaled time histories from the Peer Strong Motion Database (Pacific Earthquake Engineering Research (PEER) Center) and two time histories matched to target spectra were used to compare displacement demands.

- Recorded ground motions:
 - NGA_no_731_A10000.acc: LOMA PRIETA 10/18/89 00:05,
 - NGA_no_731_A10-UP.acc: LOMA PRIETA 10/18/89 00:05,
 - NGA_no_942-ALH090.acc: NORTHRIDGE 01/17/94
 - NGA_no_942-ALH-UP.acc: NORTHRIDGE 01/17/94
- Matched time histories are identified as:
 - Matched H1
 - Matched V

Response spectra for these input motions are shown in Figure 6. Figure 7 shows results for the ratio of displacement, δ , to seismic only displacement, δ_0 for one scenario.

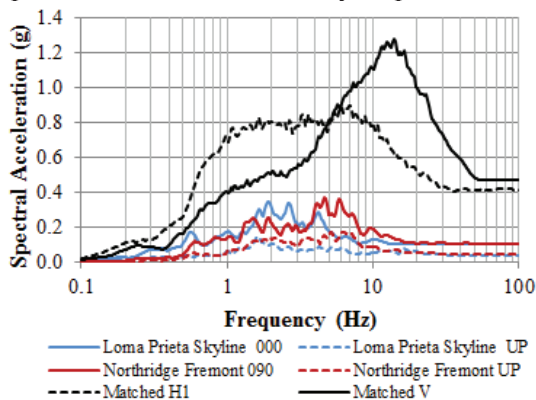


Figure 6: 5% Damped Response Spectra for Input Motions

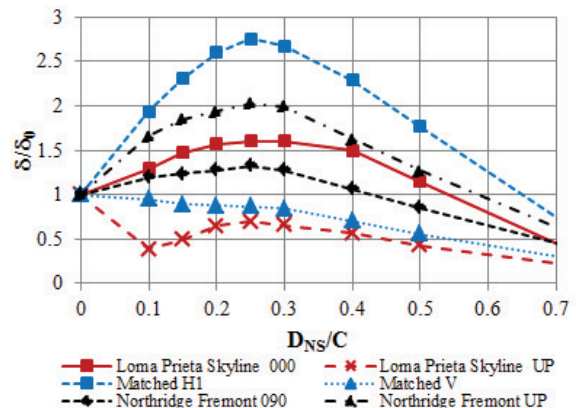


Figure 7: Displacement Ratio Results for $F_\mu = 3$, Full Hysteresis, Multiple Time Histories, 5 Hz SDOF

As shown in Figure 7, four of the time histories resulted in ratcheting responses greater than the seismic-only ductility demand while two of the time histories resulted in a reduced demand due to the partial

replacement of seismic demand with non-seismic demand. The maximum ratio of ratcheting ductility demand to seismic-only demand of 2.75 indicates significant additional ductility demand due to ratcheting in some cases. These analyses were performed for a range of inelastic energy absorption factors. Individual results were found to differ significantly by time history input motion, initial frequency of the oscillator, and value for F_{μ} , but for most sets examined, a significant portion of cases demonstrated greater ductility demand due to ratcheting.

DEVELOPMENT OF INELASTIC ENERGY ABSORPTION FACTOR REDUCTIONS

Nonlinear analyses such as those performed for this study can be used to evaluate the effect of ratcheting. However, for practical use, it is beneficial to have a more generically applicable method for use in design. As a result, additional analyses were performed to identify scaling factors appropriate for use in modifying the inelastic energy absorption factors to account for the potential for ratcheting. The analyses calculated the SDOF response for the non-ratcheting design conditions for a given value of F_{μ} to develop the code acceptable “target” ductility demand. The analyses were repeated using trial values of F_{μ} for ratcheting conditions and iterated until the new ductility demand is equal to the target ductility demand. This resulted in calculated inelastic energy absorption factors, F'_{μ} , that can be used to develop appropriate scaling factors.

The analyses were performed in the following steps:

1. Perform nonlinear SDOF analyses using the elasto-plastic backbone curve identified in Figure 1, a selected value of F_{μ} , zero non-seismic load, and seismic motions scaled to such that the demand equals the capacity C per Eq. 1. Calculate the target allowable ductility μ_{target}
2. Apply non-seismic demand (D_{NS}) consuming a given portion (γ_{ns}) of the total capacity (C), select a trial inelastic energy absorption factor value (F'_{μ}) and scale the seismic motion to consume the remaining capacity in accordance with Eq. 1. Perform the nonlinear SDOF analysis to obtain the resulting ductility, μ' .
3. Iterate the analyses until the selected value of F'_{μ} results in a ductility (μ') equaling the target ductility ($\mu' = \mu_t$).
4. Calculate the scaling factor $\alpha_{F_{\mu}}$:

$$\alpha_{F_{\mu}} = \frac{F'_{\mu} - 1}{F_{\mu} - 1} \quad \text{Eq. 3.}$$
5. Perform analysis for multiple time histories and frequencies and obtain the 16th percentile value $\alpha_{F_{\mu}}$ for various sets of analyses.

These analysis were performed for four sets of time history acceleration files:

- A set (Recorded) of 30 recorded time history motions with event magnitudes between 4.3 and 7.4 M selected from the PEER ground motion database (PEER) (Figure 8),
- A set (Set 1) of 10 time history accelerations tightly matched to one spectra with a constant acceleration target between 2 and 8 Hz and 5 time history accelerations tightly matching another spectra with a constant acceleration target between 2.5 Hz and 16 Hz (Figure 9),
- A set (Set 2) of 20 time history accelerations consisting of 20 time histories matched to a single with a relatively level acceleration between 1.5 Hz and 10 Hz (Figure 10), and
- A set (Set 3) of 10 time history accelerations matched to a target spectrum with two regions of near constant acceleration (Figure 11).

The recorded set is intended to represent real motions. Set 1 best represents constant acceleration regions and Set 2 and Set 3 were included to increase the quantity of data examined. For each of these sets of time histories, the above analysis was performed to determine the scaling factor $\alpha_{F_{\mu}}$ considering $F_{\mu} = 2, 3$,

4, and 5 and at 30 frequencies at 0.5 Hz increments from 1 Hz to 15 Hz. These analyses produced substantial quantity of data.

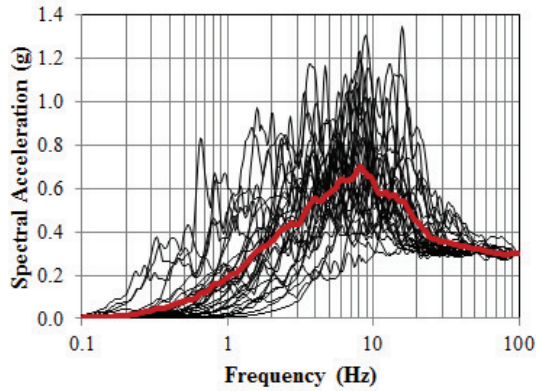


Figure 8: Response spectra for 30 recorded time histories scaled to 0.3g PGA (thick red line = average of 30)

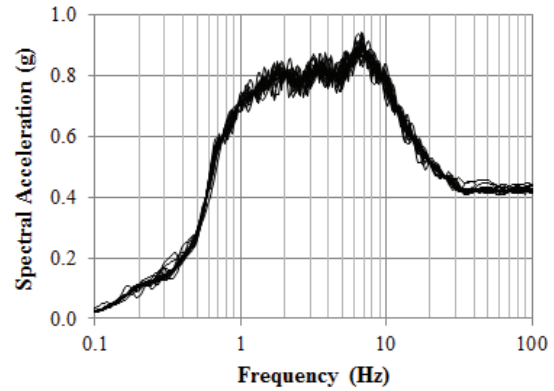


Figure 10: Response Spectra for Time Histories in Set 2

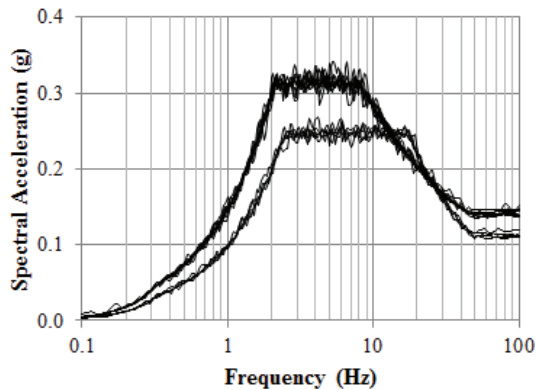


Figure 9: Response Spectra for Time Histories in Set 1

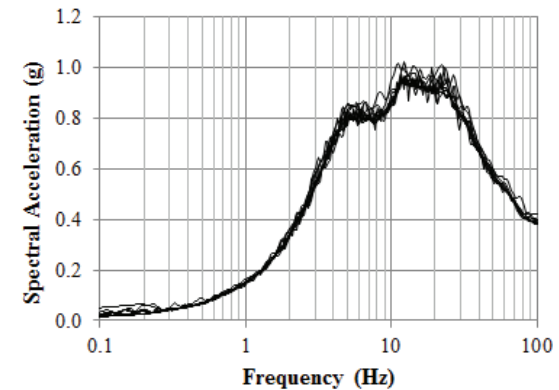


Figure 11: Response Spectra for Time Histories in Set 3

Figure 12 shows an example of results for analyses performed for the Recorded set of ground motions and the full hysteresis model. Each line connects results from each time history in the set. Median and 16th percentile results at each frequency are also shown. The nonlinear behavior resulted in a large variation between responses for different input motions and different frequencies for the same input motions. Because of this variation, the results were treated probabilistically with a target of 84th percentile non-exceedance equivalent to 16th percentile value for $\alpha_{F\mu}$. Figure 13 shows median and Figure 14 shows the 16th percentile value for $\alpha_{F\mu}$ for each of the 4 sets of time histories for a design $F_{\mu} = 3$. The ratcheting effect on ductility demand appears to reduce in the higher frequency range, particularly for Set 2. This reduction in ratcheting effect could be related to the shape of the input spectra. Input motions from Set 2 begin to reduce in spectral acceleration above 8 Hz and ratcheting appears to be less significant in this region. Set 1 results show a similar, but less pronounced, trend, as only two-thirds of the input motions reduce spectral accelerations above 8 Hz, and the rest stay constant up to almost 20 Hz. Similar change in $\alpha_{F\mu}$ is not observed for the low frequency regions.

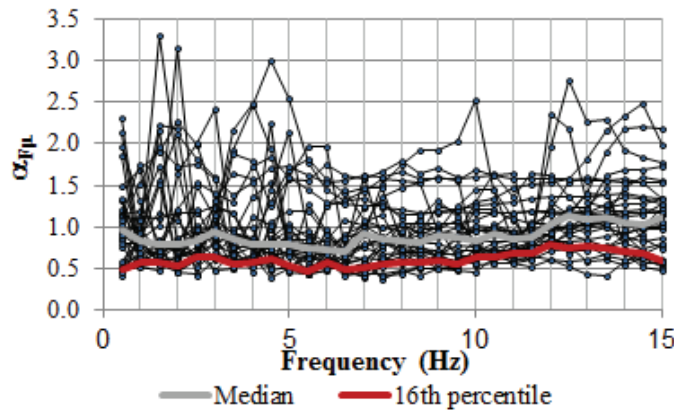


Figure 12: Ratio $\alpha_{F\mu}$ for Recorded Set of Time Histories at $F_\mu = 3$, 20% Non-Seismic Demand (Full Hysteresis)

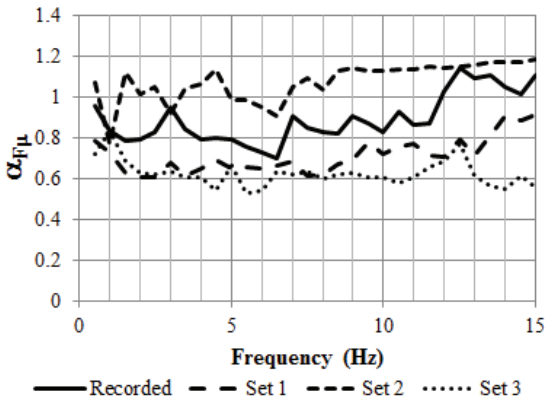


Figure 13: Median ratio $\alpha_{F\mu}$ for 4 sets of Time Histories at $F_\mu = 3$, 20% Non-Seismic Demand (Full Hysteresis)

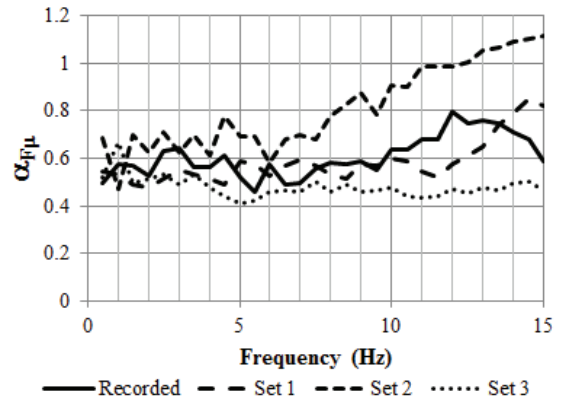


Figure 14: Ratio $\alpha_{F\mu}$ (16th percentile) for 4 sets of Time Histories at $F_\mu = 3$, 20% Non-Seismic Demand (Full Hysteresis)

Figure 15 shows the calculated value for $\alpha_{F\mu}$ over a range of non-seismic demand ratios at a value of $F_\mu = 3$. The effect of non-seismic demand on $\alpha_{F\mu}$ is most significant between about 10% and 30% non-seismic demand.

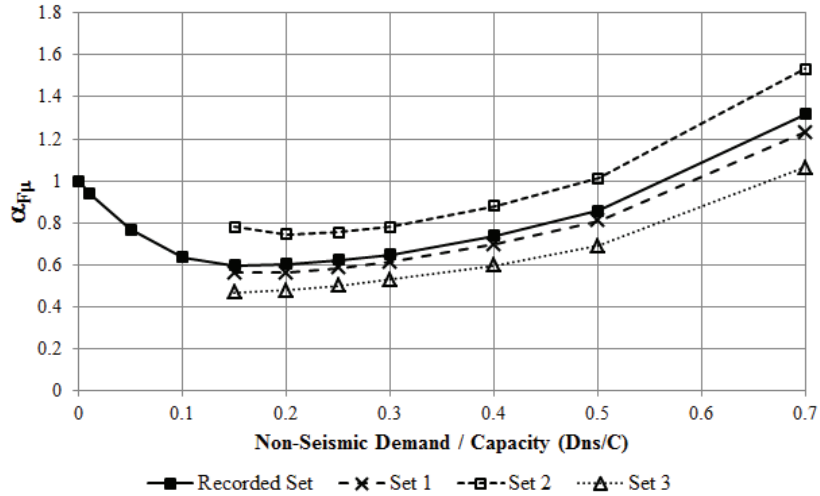


Figure 15: Ratio $\alpha_{F\mu}$ (16th percentile) for 4 sets of Time Histories at $F_{\mu} = 3$ (Full Hysteresis)

For the cases considered, significant differences exist between the sets of motion examined in addition to variation within the sets. It is not clear if these differences are a result of small sample size or if there is a characteristic of the time histories, such as strong motion duration or Fourier frequency content, causing the difference. The recorded motions produce results similar to that of Set 1 and between Set 2 and Set 3. Since the recorded time history results are of a similar magnitude as the matched time histories and recorded motions are unaffected by the matching processes, only the recorded motions were used in developing the results further.

Figure 16 shows the value $\alpha_{F\mu}$ for the set of recorded motions over a range of non-seismic demand ratios and for various values of F_{μ} . These results show that $\alpha_{F\mu}$ is relatively constant between about 10% and 40% non-seismic demand and that the results are reasonably similar for F_{μ} values 3 and above. At low values for F_{μ} , the effect of F_{μ} is less significant to the design.

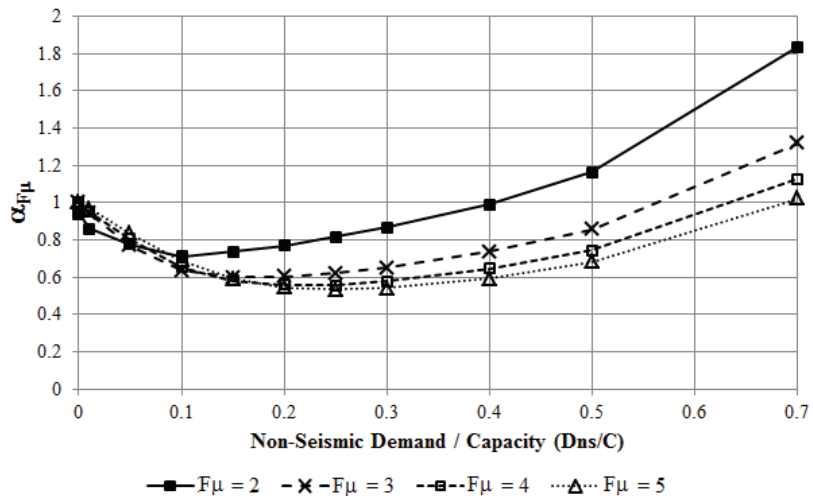


Figure 16: Ratio $\alpha_{F\mu}$ (16th percentile) for Set of Recorded Time Histories (Full Hysteresis)

Analyses performed with the pinched concrete hysteresis model demonstrate similar response as the full hysteresis model, but the overall effect on ductility demand is reduced. The effect on the calculation of $\alpha_{F\mu}$ is shown in Figure 17.

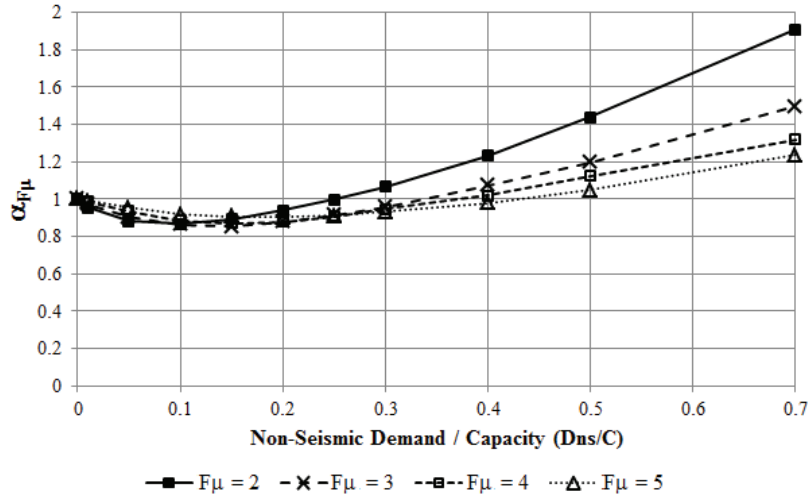


Figure 17: Ratio $\alpha_{F\mu}$ (16th percentile) for Set of Recorded Time Histories (Pinched Hysteresis)

CONCLUSION AND RECOMMENDATION

The above analysis results can be reasonably used to provide adjustment factors to account for ratcheting in design analyses. It is beneficial to provide simplified approaches rather than detailed analysis for this purpose. The authors propose the following approach to adjust the inelastic energy absorption factor in accordance with Equation 3 to obtain an 84th percentile condition for non-exceedance of the non-ratcheting ductility. Adjust inelastic energy absorption factors according to Eq. 4:

$$F'_\mu = \alpha_{F\mu} \cdot (F_\mu - 1) + 1 \quad \text{Eq. 4.}$$

Where:

F'_μ is the effective inelastic energy absorption factor to be applied to account for ratcheting effects,
 F_μ is the original inelastic energy absorption factor developed without consideration for ratcheting,
 and,

$\alpha_{F\mu}$ is the ratcheting inelastic energy absorption factor adjustment coefficient. The coefficient is dependent on the ratio of non-seismic demand, D_{NS} , to code capacity, C , as follows:

$$\alpha_{F\mu} = 1 \text{ for } D_{NS}/C = 0$$

$$\alpha_{F\mu} = 0.6 \text{ for } 0.1 \leq D_{NS}/C \leq 0.4$$

$$\alpha_{F\mu} = 1, \text{ for } D_{NS}/C \geq 0.6$$

Linear interpolation shall be used to determine values of $\alpha_{F\mu}$ for intermediate values of D_{NS}/C .

When F_μ is less than 3, linear interpolation may be used between a value of 1 at $F_\mu = 1$ and the above values at $F_\mu = 3$.

Although this recommendation does not envelop the entire set of 16th percentile results calculated, the approach provides simplicity and a rational approach to account for increased ductility demand due to ratcheting. No recommendation is provided for pinched concrete hysteresis because only one concrete model was examined, but the recommendation for full hysteresis appears to be conservative for pinched concrete models.

REFERENCES

- ASCE/SEI Standard 43-05. (ASCE/SEI 43-05) "Seismic Design Criteria for Structures, Systems, and Components in Nuclear Facilities," American Society of Civil Engineers and Structural Engineering Institute, Reston, VA.
- ASCE Standard 7-10. (ASCE 7) "Minimum Design Loads for Buildings and Other Structures," American Society of Civil Engineers, Reston, VA.
- Ibarra, Luis F., Ricardo a. Medina, and Helmut Krawinkler. (2005) "Hysteretic Models That Incorporate Strength and Stiffness Deterioration." *Earthquake Engineering & Structural Dynamics* 34 (12) (October), 1489–1511.
- Mertz, Greg E., and Tom Houston. (2001) "Force Reduction Factors for the Structural Design and Evaluation of Facilities Containing Nuclear and Hazardous Materials (U) (WSRC-TR-2001-00037 Revision 0)." Aiken, SC.
- Pacific Earthquake Engineering Research Center. (PEER) "PEER Ground-Motion Database." http://peer.berkeley.edu/products/strong_ground_motion_db.html. Berkeley, CA.